

Ultraviolet HST Observations of the Jet in M87¹

Christopher Z. Waters and Stephen E. Zepf

Department of Physics and Astronomy, Michigan State University, East Lansing, MI 48824

watersc1@pa.msu.edu, zepf@pa.msu.edu

ABSTRACT

We present new ultraviolet photometry of the jet in M87 obtained from HST WFPC2 imaging. We combine these ultraviolet data with previously published photometry for the knots of the jet in radio, optical, and X-ray, and fit three theoretical synchrotron models to the full data set. The synchrotron models consistently overpredict the flux in the ultraviolet when fit over the entire dataset. We show that if the fit is restricted to the radio through ultraviolet data, the synchrotron models can provide a good match to the data. The break frequencies of these fits are much lower than previous estimates. The implied synchrotron lifetimes for the bulk of the emitting population are longer than earlier work, but still much shorter than the estimated kinematic lifetimes of the knots. The observed X-ray flux cannot be successfully explained by the simple synchrotron models that fit the ultraviolet and optical fluxes. We discuss the possible implications of these results for the physical properties of the M87 jet. We also observe increased flux for the HST-1 knot that is consistent with previous results for flaring. This observation fills in a significant gap in the time coverage early in the history of the flare, and therefore sets constraints on the initial brightening of the flare.

Subject headings: galaxies: active – galaxies: individual (M87) – galaxies: jets – magnetic fields – radiation mechanisms: nonthermal

1. Introduction

M87 is one of the closest galaxies hosting a prominent jet. Its location in the core of the Virgo cluster at a distance of 16 Mpc (e.g. Macri et al. 1999) makes M87 close enough that

¹Based on observations made with the NASA/ESA Hubble Space Telescope, obtained at the Space Telescope Science Institute, which is operated by the Association of Universities for Research in Astronomy, Inc., under NASA contract NAS 5-26555.

the structure of the jet can be resolved by space-based observations. It has been studied extensively from the radio (e.g., Sparks et al. 1996, Biretta et al. 1995) to X-ray (e.g., Marshall et al. 2002, Wilson & Yang 2002), with many broadband studies in the optical (e.g. Perlman et al. 2001, Biretta et al. 1991). In addition to photometric surveys of the jet, polarimetry maps of the jet have been created (Perlman et al. 1999), and the bulk motion of the jet has been investigated by measuring the proper motions of the jet’s component knots over decade-long observation programs (Biretta et al. 1995). All of these observations have provided more information about M87 than is known for nearly any other extragalactic jet.

However, there have been no far ultraviolet observations with spatial resolution sufficient to resolve the structure of the jet in detail. These observations are essential for constraining the synchrotron emission, because the break frequencies of the models fit to extant data are between the optical and X-ray. Moreover, the different models that fit the radio, optical, and X-ray data make significantly different predictions for the shape of the spectrum in the ultraviolet.

In this paper, we use high spatial resolution ultraviolet images obtained with HST to address questions about the physical characteristics of the emission from the M87 jet. In Section 2, we present these observations and detail the reduction process. We compare our measurements to theoretical models of the jet emission in Section 3. In Section 4 we discuss the evidence for flaring in our observations of HST-1, and use this to constrain the early evolution of this flare. We summarize our conclusions in section 5.

2. Observations and Analysis

The jet of M87 was observed with the WFPC2 detector aboard HST on 2001 February 23. The galaxy core was centered in the PC, with the jet oriented along the columns of the detector. The observations were obtained through the F170W filter, which has an effective wavelength of 1666Å. Six images were taken in an “L” shaped dither pattern with 0’25 shifts between the positions. The total integration time of the observations was 7600 seconds.

We combined the six observations with the Dither package in IRAF, using the DRIZZLE algorithm from Fruchter & Hook (2002). This both cleans the final image of cosmic rays and CCD flaws and takes advantage of the subpixel spacing between image positions to construct a final image with smaller pixels. The Dither package also corrects the input images for the geometric distortion of the WFPC2, which is largest in the ultraviolet.

The knots of the jet were photometered based on the apertures defined by Perlman et

al. (2001) in their study of HST optical images of the jets. We have chosen to use the same apertures to allow direct comparison of our fluxes with those presented. The boundaries of our apertures are defined by finding the closest pixel boundary that matches the positions listed by Perlman. In order to ensure that the core of the galaxy does not interfere with any of the knots, we have removed the galaxy profile using the ISOPHOTE package in IRAF. Only knot HST-1 has any possible contribution from the core, as there is little evidence of the galaxy beyond $0''.55$ from the core.

The photometry determined within these apertures was calibrated using the default values for the F170W filter given in the WFPC2 Calibration Manual (Baggett et al. 2002). Because our images have low background levels, we need to account for possible charge transfer efficiency losses. We calculated the correction using methods from both Whitmore, et al. (1999) and Dolphin (2000). As the results were similar, we used the average of the two methods as our final correction, and the difference between the methods as the uncertainty for this correction. Since both of these methods are based on the assumption of a point source object, we adopted the suggestion presented in Riess (2000) to half the calculated correction. The typical level of this correction was about 10%. Another possible concern is the effect of contaminants on the WFPC2 is generally worse in the UV than at other wavelengths. For this set of observations, the WFPC2 had been decontaminated less than a week prior, so the correction we applied is less than 2% of the measured counts. We used no aperture correction for these measurements, as our apertures extend well beyond the visible portions of the knots. The final fluxes, along with the distance from the core for each knot are listed in Table 1.

Table 1. Photometric Data

Knot	F(F170W) (μJy)	Distance (arcsec)
HST-1	15.8 ± 0.6	1.25
D	26.7 ± 0.9	3.45
D-East	17.8 ± 1.1	2.85
D-Mid	4.7 ± 0.4	3.52
D-West	5.7 ± 0.5	3.52
E	10.0 ± 0.9	6.30
F	34.5 ± 1.7	8.72
I	11.3 ± 1.4	11.19
A	275.2 ± 12.7	12.67
A-bar	15.3 ± 2.9	11.80
A-shock	166.2 ± 9.6	12.40
A-diff	86.9 ± 6.7	13.28
B	147.4 ± 7.9	14.98
B-1	83.9 ± 6.5	14.41
B-2	44.3 ± 3.9	15.59
C-1	80.8 ± 12.9	17.53

3. Comparison to Models

We combined our ultraviolet photometry with published radio and optical data from Perlman et al. (2001) and X-ray data from Marshall et al. (2002). We chose three standard theoretical synchrotron models to fit to the data. The KP model (Kardashev 1962; Pacholczyk 1970) assumes that the source of the emission is a single burst of energetic electrons with an isotropic pitch angle distribution. The pitch angle distribution of this model is not allowed to vary, so some high energy electrons can remain with trajectories nearly parallel to the magnetic field. Although this model is physically unlikely, as relativistic electrons are known to scatter, we include this model in our fits to compare with previously published results using this model. The JP model (Jaffe & Perola 1973) also assumes a single burst of electrons with an isotropic pitch angle distribution, but allows the pitch angle distribution to scatter so that it always has an isotropic distribution. This allows all high energy electrons to quickly radiate away their energy, resulting in an exponential falloff beyond the break frequency. We also consider a continuous injection (CI) model of Heavens & Meisenheimer (1987) in which energetic electrons are being constantly added to the emitting region. Although other synchrotron models have been considered for M87 (e.g. Coleman & Bicknell 1988), these models are the most common for comparison to the data, and are likely to bracket the range of physical possibilities.

The synchrotron fitting to the data was performed using new code based on a program provided by Chris Carilli (Carilli et al. 1991). Our code determines the best fitting low frequency power law index, break frequency, and intensity scaling to the data using the Levenberg-Marquardt algorithm implementation in the GNU Scientific Library¹. Using this procedure, we determine the best fit parameters for each model over the full spectral range. These best fit values, along with the reduced chi-squared values for each knot fit are listed in Table 2. For reference, the kinematic ages calculated from the proper motions (Biretta et al. 1995) of the knots are listed where available. The final calculated best fitting model SEDs are shown in the left panels of Figure 1.

The models described above appear to be unable to fit the full optical, ultraviolet and X-ray spectrum for many of the knots. They systematically overpredict our far UV flux, and to a lesser extent, the previously published near ultraviolet (F300W) data. The flux in the ultraviolet also appears to drop below the simple power-law form produced by synchrotron models at frequencies well below the break frequency. This ultraviolet turnover suggests that we are close to the break frequency for a synchrotron model that fits the radio to ultraviolet data. If this is the case, then the X-ray flux is higher than the prediction for a

¹<http://www.gnu.org/software/gsl/>

simple synchrotron model, and it would seem that this fact is forcing our code to choose higher break frequency models, despite their poor fit in the ultraviolet. By refitting the models without the X-ray flux, we can generate models that are much better fits to the radio through ultraviolet emission. The best fitting parameters for these new fits are given in table 3, and the new synchrotron fits are shown in the right panels of Figure 1. These fits provide much lower break frequencies for the emission, and for the three knots with obvious ultraviolet turnovers (knots D, A, and B), these fits have much lower χ^2 values compared to those generated using the X-ray measurement. The remaining two knots (knots E and F), have minimal difference in the fit quality, which suggests that we still do not have direct measurements around the break frequency.

If the radio through far UV emission is generated by a single burst synchrotron model, then the excess of X-ray flux compared to these models must be accounted for. Inverse Compton is a tempting option, as it has been used to explain X-ray emission in other jets. However, previous analysis has shown that the geometry of the jet required for inverse Compton to contribute significantly to the X-ray flux from the knots is inconsistent with the geometry indicated by proper motion studies. Specifically, the beaming model presented by Harris & Krawczynski (2002) predicts that in order to explain the observed X-ray flux, the angle of the jet to the line of sight must be nearly zero, in contradiction to the 20° value derived from proper motions (Biretta et al. 1999). It is clear then that there must be some reinjection or re-excitation of electrons in the emitting regions. This scenario has some direct evidence to support it. The kinematic ages of the knots in the jet are much longer than the calculated synchrotron ages. Therefore, even to explain the optical emission of the jet, some amount of fresh high energy material from shocks along the jet must be added.

Table 2. Parameters for Synchrotron Model Fits for Radio through X-ray Data

	HST-1	D	E	F	A	B
$T_{kin}(\text{yr})$		2037		2500	6169	6353
KP: α	0.711	0.706	0.703	0.671	0.670	0.651
$\nu_B(\text{Hz})$	7.52×10^{15}	5.15×10^{16}	4.32×10^{16}	8.80×10^{15}	1.22×10^{16}	2.71×10^{15}
χ^2	3.22×10^3	39.1	8.91	11.1	14.4	3.21
$\tau_{sync}(\text{yr})$	386	148	161	357	303	643
JP: α	0.718	0.708	0.706	0.686	0.683	0.699
$\nu_B(\text{Hz})$	1.00×10^{16}	1.24×10^{17}	1.12×10^{17}	6.35×10^{16}	6.99×10^{16}	5.21×10^{16}
χ^2	1.29×10^4	42.1	9.48	15.4	32.4	54.2
$\tau_{sync}(\text{yr})$	335	95	100	134	127	147
CI: α	0.705	0.683	0.711	0.804	0.741	0.855
$\nu_B(\text{Hz})$	1.56×10^{21}	9.27×10^{14}	1.22×10^{15}	8.75×10^{14}	7.60×10^{14}	6.48×10^{14}
χ^2	37.2	44.3	83.6	5.62×10^3	2.86×10^3	2.65×10^4
$\tau_{sync}(\text{yr})$	1	1100	959	1132	1214	1315

Table 3. Parameters for Synchrotron Model Fits for Radio through Ultraviolet Data

	D	E	F	A	B
KP: α	0.668	0.690	0.664	0.641	0.645
$\nu_B(\text{Hz})$	3.07×10^{15}	9.77×10^{15}	5.61×10^{15}	2.66×10^{15}	1.90×10^{15}
χ^2	9.81	8.23	12.7	3.15	0.54
$\tau_{sync}(\text{yr})$	604	339	447	649	768
JP: α	0.668	0.690	0.664	0.642	0.646
$\nu_B(\text{Hz})$	5.36×10^{15}	1.68×10^{16}	9.70×10^{15}	4.70×10^{15}	3.43×10^{15}
χ^2	9.63	8.22	12.7	3.04	0.50
$\tau_{sync}(\text{yr})$	457	258	340	488	572
CI: α	0.668	0.690	0.664	0.639	0.636
$\nu_B(\text{Hz})$	1.19×10^{15}	4.22×10^{15}	2.32×10^{15}	9.43×10^{14}	5.10×10^{14}
χ^2	11.9	8.35	13	4.27	1.82
$\tau_{sync}(\text{yr})$	971	515	695	1090	1483

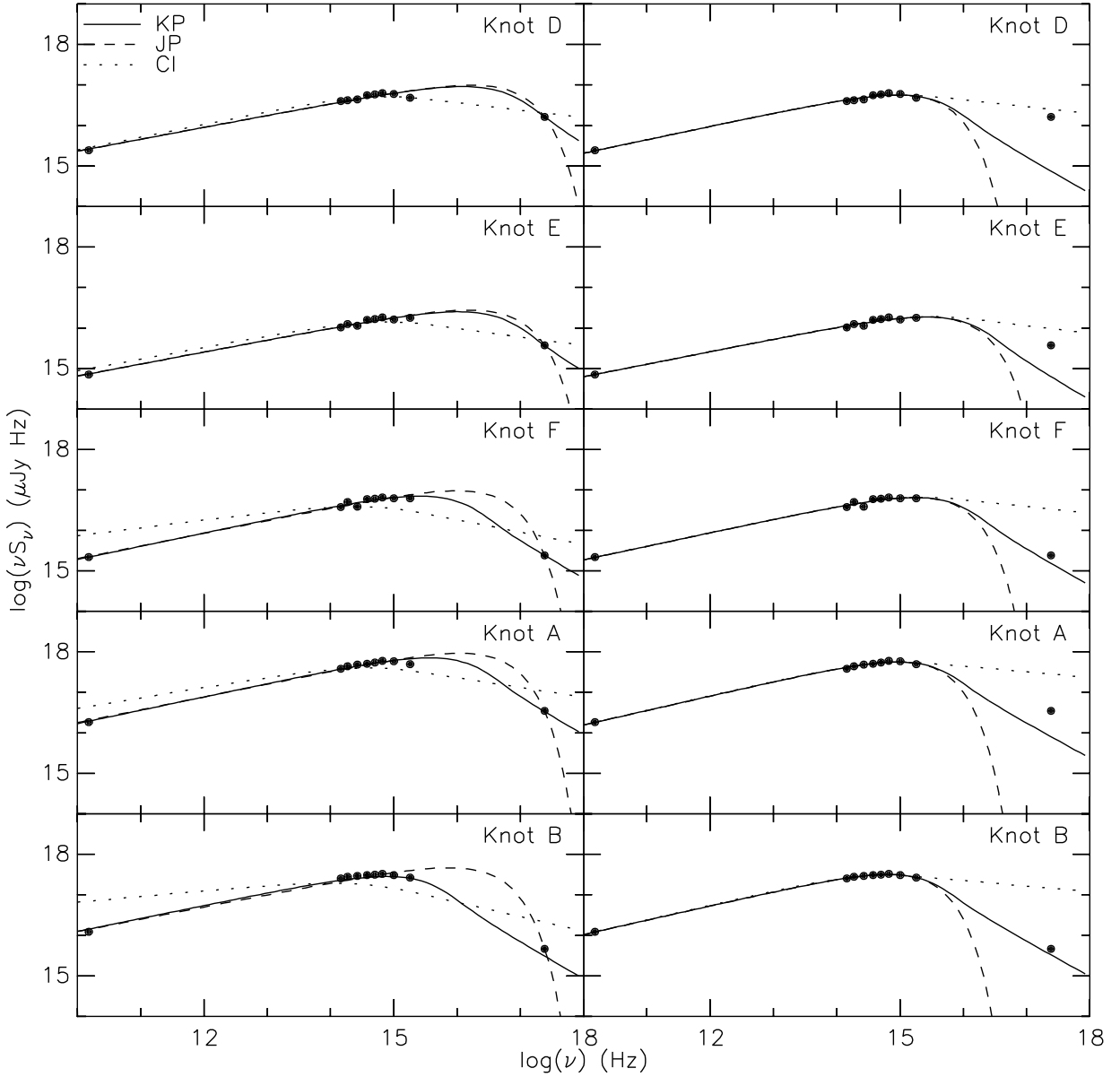


Fig. 1.— A plot of the spectral energy distributions for the knots of the jet from radio through X-ray wavelengths. The data are plotted as points, and the best fits for each of the synchrotron models are plotted as shown above. The error bars for the fluxes are smaller than the points used. The left panel displays model fits that include the X-ray data, and the right panel shows the fits without these data. The left panel demonstrates that the models are unable to fit both the turnover from the power law seen in the ultraviolet and the X-ray data point. The right panel shows that the synchrotron models with much lower break frequencies can provide a reasonable fit to the radio through ultraviolet data. The best fitting parameters of these models are listed in Table 2 and Table 3

4. Flaring Outburst of HST-1

HST-1, the knot closest to the core of M87, has been shown to have a very dynamic light curve (Perlman et al. 2003; Harris et al. 2003). Observations from late 2001 to the present show a significant increase in the brightness of HST-1 compared to initial optical observations on 1999 May 11 and 1998 February 25 (Perlman et al. 2001, 2003), along with shorter timescale variability. As can be seen in the right panel of Figure 2, our observation of HST-1 obtained in February 2001 fills a significant gap in the light curve of the flare, and thus it is interesting to examine our data to help constrain the early evolution of the flare.

By comparing our ultraviolet photometry for HST-1 to the synchrotron model fits of earlier optical coeval data (Perlman et al. 2001) we can immediately note that our observation is substantially brighter than expected from these earlier data, as shown in the left panel of Figure 2. As the fluxes for the other knots in the jet tend to either lie in agreement with the synchrotron fits, or suggest a drop in the ultraviolet, it is unlikely that this brightening is a result of an error in the data reduction. This suggests that our observation shows that HST-1 has begun its flaring outburst by the time of our observations.

To make a quantitative comparison to the many observations of knot HST-1 obtained at different times, we need to convert all measurements to the flux at a standard wavelength. We follow previous work on this flare (Perlman et al. 2003) and adopt a power law index of $\alpha = 0.6$ to scale our measurement to a standard wavelength of 2200\AA . Applied to our data through the F170W filter gives a flux of $F_{220nm} = 18.67 \pm 0.71 \mu\text{Jy}$ in our measurement on 2001 February 23. A plot of this measurement and those of the flare of HST-1 at other times are shown in figure 2b. Our data requires the flare to have begun before February 2001, significantly pushing back the earliest observation of the flare. Adopting a simple exponential function to fit the initial rise of the flare gives a flux doubling time scale for the beginning of the flare of 283 days, consistent with other previously published timescales, and constrains the start of the flare to February 2000.

The flaring emission in HST-1 arises from the upstream edge of the knot. This region is consistent with a source size below our resolution limit, giving us a maximum size for the flaring region of 1.8pc. If we assume that our flux doubling timescale is on the order of the light crossing time, then we can set an upper limit on the Doppler factor for the emission region of $\delta \lesssim 8$, as a value any larger would allow us to resolve the source of the flare. This result is consistent with multiwavelength results presented in Perlman et al. (2003), where a more detailed analysis has been done of the constraints the variability places on the physical structure of the inner jet. However, as their results are also resolution limited, it seems clear that higher resolution imaging is required to further constrain the size of the flaring outburst.

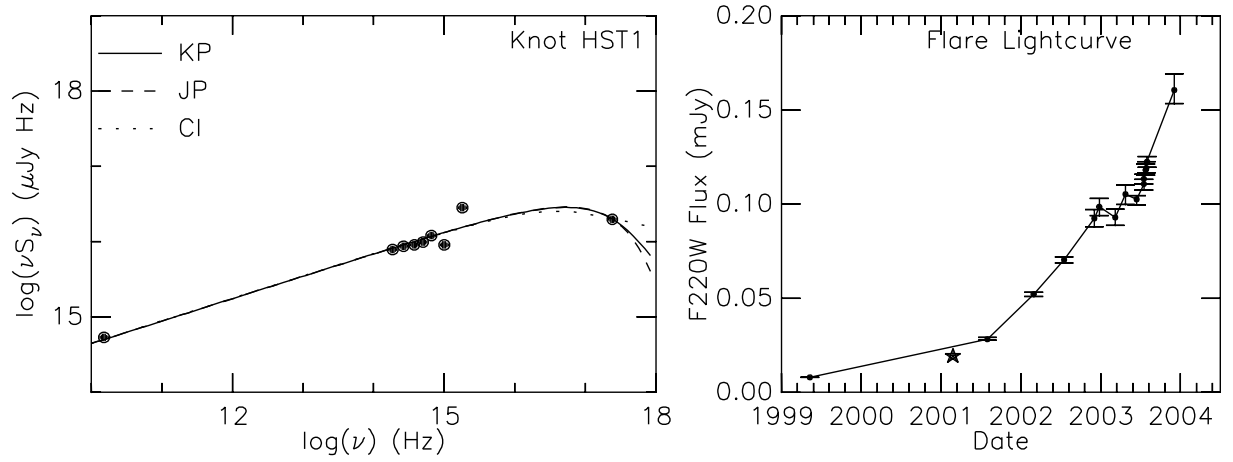


Fig. 2.— Best fitting synchrotron SED for HST-1. The new UV point can be seen to exceed the fit by a large amount. The right panel shows the light curve for the knot HST-1 based on data from Perlman (private communication). The new data point is plotted as a star.

5. Discussion

The standard synchrotron models that are used to fit extragalactic jets all predict a power law from the radio through the optical, and have a break in the emission somewhere between ultraviolet and X-ray frequencies. These models can readily fit both the optical power law and an X-ray measurement by simply choosing a sufficiently high break frequency. The ultraviolet flux predicted by these fits is high, as the power law extends into the ultraviolet for such high break frequencies. However, our ultraviolet observations of the knots of the M87 jet have shown that we have detected a turnover in the spectrum for knots D, A, and B. The break frequencies that accurately model these turnovers are much lower than those previously determined to fit the X-ray flux. This leads to a problem in using these existing synchrotron models to fit the full radio to X-ray spectrum.

The single burst models we have considered significantly underpredict the X-ray flux with the lower break frequencies required by the ultraviolet data. The CI model has the opposite problem, as it overpredicts the X-ray flux. For the majority of the knots, the spectral break is much larger than that predicted by the CI model, consistent with the steep X-ray spectra found by Wilson & Yang (2002). Only knot D has a spectral break close to the CI model prediction of $\Delta\alpha = 0.5$. The X-ray data from Wilson & Yang (2002) also indicates that the emission peak for the X-ray data is further upstream than the optical and radio emission peaks. This observation supports a scenario in which the electrons are shocked at the upstream edge of the knot, and then spectrally age as they travel downstream. Therefore, the fact that the CI model does not accurately predict the high frequency behavior may suggest that the properties in the emitting region are not as static as the CI model assumes. Changes in the downstream properties like those studied by Coleman & Bicknell (1988) can give rise to large breaks similar to what we measure.

Another possible explanation for the observed spectra arises from allowing the number of electrons excited to vary over time. The JP model with its single burst, and the continuous injection of the CI model can be considered limiting cases of such a variation. As the observed spectra are intermediate between these two models, but lie closer to that predicted by the CI model, it is possible that the shock fronts simply do not always excite the same number of electrons. The flaring emission of knot HST-1 indicates that the emission from the shock is not necessarily constant in time, and that variation in the shock as well as downstream may contribute to the deviations from the theoretical model. Our observation of this knot helps to constrain the early evolution of the flare, suggesting a start date for the flare in early February 2000, and giving a doubling time scale of 0.77 years, similar to that found at later times for the flare. This flaring behavior illustrates that the emission of the knots in the jet is influenced by shocks on scales smaller than the observed sizes of the knots.

We thank E. Perlman for helpful discussions and for supplying data for the light curve of knot HST-1 and C. Carilli for making his synchrotron fitting code available. We also thank the anonymous referee for helpful comments and discussion. This work was supported by NASA through grant HST-GO-08725-05-A and awarded by the Space Telescope Science Institute, which is operated by the Association of Universities for Research in Astronomy, Inc., for NASA under contract NAS5-26555.

REFERENCES

- Baggett, S., et al., 2002, HST WFPC2 Data Handbook, v. 4.0 (Baltimore: STSci)
- Biretta, J. A., Stern, C. P., & Harris, D. E., 1991, *AJ*, 101, 1632
- Biretta, J. A., Zhou, F., & Owen, F.N., 1995, *ApJ*, 447, 582
- Biretta, J. A., Sparks, W. B., & Macchetto, F., 1999, *ApJ*, 520, 621
- Carilli, C. L., Perley, R. A., Dreher, J. W., & Leahy, J. P., 1991, *ApJ*, 383, 554
- Coleman, C. S., & Bicknell, G. V., 1988, *MNRAS*, 230, 497
- Dolphin, A. E., 2000, *PASP*, 112, 1397
- Fruchter, A. S., & Hook, R. N., 2002, *PASP*, 114, 144
- Harris, D. E., & Krawczynski, H., 2002, *ApJ*, 565, 244
- Harris, D. E., Biretta, J. A., Junor, W., Perlman, E. S., Sparks, W. B., & Wilson, A. S., 2003, *ApJL*, 586, L41
- Heavens, A. F., & Meisenheimer, K., 1987, *MNRAS*, 225, 335
- Jaffe, W. J., & Perola, G. C., 1973, *A&A*, 26, 423
- Kardashev, N. S., 1962, *SvA (AJ)*, 6, 317
- Macri, L. M., et al., 1999, *ApJ*, 521, 155
- Marshall, H. L., Miller, B. P., Davis, D. S., Perlman, E. E., Wise, M., Canizares, C. R., & Harris, D. E., 2002, *ApJ*, 564, 683
- Pacholczyk, A. G., 1970, *Radio Astrophysics* (San Francisco: Freeman)
- Perlman, E. S., Biretta, J. A., Zhou, F., Sparks, W. B., & Macchetto, F. D., 1999, *AJ*, 117, 2185
- Perlman, E. S., Biretta, J. A., Sparks, W. B., Macchetto, F. D., & Leahy, J. P., 2001, *ApJ*, 551, 206
- Perlman, E. S., Harris, D. E., Biretta, J. A., Sparks, W. B., & Macchetto, F. D., 2003, *ApJL*, 599, L65
- Sparks, W. B., Biretta, J. A., & Macchetto, F., 1996, *ApJ*, 473, 254

Riess, A., 2000, WFPC2 Instrument Sci. Rep. 00-04 (Baltimore: STSci)

Whitmore, B., Heyer, I., & Casertano, S., 1999, PASP, 111, 1559

Wilson, A. S., & Yang, Y., 2002, ApJ, 568, 133